Journal of Applied Polymer Science

Controllable preparation of a soluble trapezoidal polyacetylene with broadband absorption by a one-step strategy

Fayin Zhang,[1] Shanyi Guang,[2] Gang Wei,[1] Gang Zhao,[1] Fuyou Ke,[1] Yihu Feng,[1] Hongyao Xu[1]

[1]The State Key Laboratory for Modification of Chemical Fibers and Polymer Materials, College of Materials Science and Engineering, Donghua University, Shanghai 201620, China

[2]College of Chemistry and Bioengineering, Donghua University, Shanghai 201620, China

Correspondence to: H. Xu (E-mail: hongyaoxu@163.com)

ABSTRACT: A new trapezoidal functional polyacetylene with broadband absorption from the visible to the near infrared and excellent thermal stability was effectively prepared by molecular design and a controllable strategy. It is completely soluble in common organic solvents because the 6-ethynyl-2-methylquinoline copolymerized with phenylacetylene. The absorption spectrum can be effectively adjusted by controlling the ratio of semi-squaraine and squaraine in the process of preparation. Interestingly, it was found that the improvement of thermal stability of the target product may originate from the synergy of the shielding effect of the quinoline ring to the main chain and the strong interactions between squaraine groups. The formation mechanism of the broadband absorbance properties was studied through an online spectrum tracking method. © 2016 Wiley Periodicals, Inc. J. Appl. Polym. Sci. **2016**, *133*, 44096.

KEYWORDS: copolymers; dyes and pigments; functionalization of polymers

Received 14 April 2016; accepted 17 June 2016
DOI: 10.1002/app.44096

INTRODUCTION

Polyacetylene, a prototypical conjugated polymer, has attracted considerable interest owing to its large third-order nonlinear optical properties,[1,2] good conductivity, and fast response time.[3–5] In recent years, it was found that functionalized polyacetylenes have many unique advantages compared to other polymers and have been applied in many fields, including photoluminescence,[6] electroluminescence,[7] p-n heterojunctions,[8] bioactivity,[9] and image sensors.[10] However, the strong π-π stacking interactions between conjugated structures often result in the formation of fibrillar crystals and low solubility, poor processing performance, and instability in the air, which have significantly limited the scope of its applications.[11–15] Suitable molecular designs have not only improved its solubility but also have endowed polyacetylene with some novel properties.

In our previous work, soluble polyacetylenes containing chromophores with different conjugation bridge structures or terminal substituents were designed and prepared successfully.[16] Soluble polyacetylenes bearing oxadiazole groups with two novel, high molecular weights were also prepared.[17,18] Recently, disubstituted liquid crystalline polyacetylene containing a 4-nonyloxy phenyl group or a flexible alkyl spacer with lyotropic and thermotropic liquid crystal behaviors was reported.[19] Optically active amphiphilic polymer brushes on helical polyacetylene as a class of polymeric architectures containing a long backbone and densely grafted side chains have attracted much attention because of their special structures and properties.[20,21] Even optically active and magnetic microparticles consisting of substituted polyacetylene/Fe_3O_4 nanoparticles can be used as a chiral additive to induce enantioselective crystallization.[22] In our group, some fluorine-containing polyacetylenes with near-infrared properties were successfully prepared.[23] However, polyacetylene with broadband absorption has rarely been reported.[24]

Semi-squaraine and squaraine have aroused large interest because of their excellent photoelectric properties, strong broadband absorption, high stability, and easy modification of the structure. Consequently, they were widely applied in the detection of metal ions,[25–27] in biological detection,[28] and in solar cells.[27–30]

In this paper, squaraines were incorporated into polyacetylene to form soluble trapezoidal polyacetylene with broadband absorption by a one-step strategy. To improve the solubility, phenylacetylene was copolymerized with methyl quinoline acetylene to obtain some interesting properties, such as high molecular weight and good solubility. Then, polyacetylene with broadband absorption was synthesized by a one-step strategy from P 1 to P 2 (Figure 1). This method not only ensures a functional polyacetylene with high

Additional Supporting Information may be found in the online version of this article.

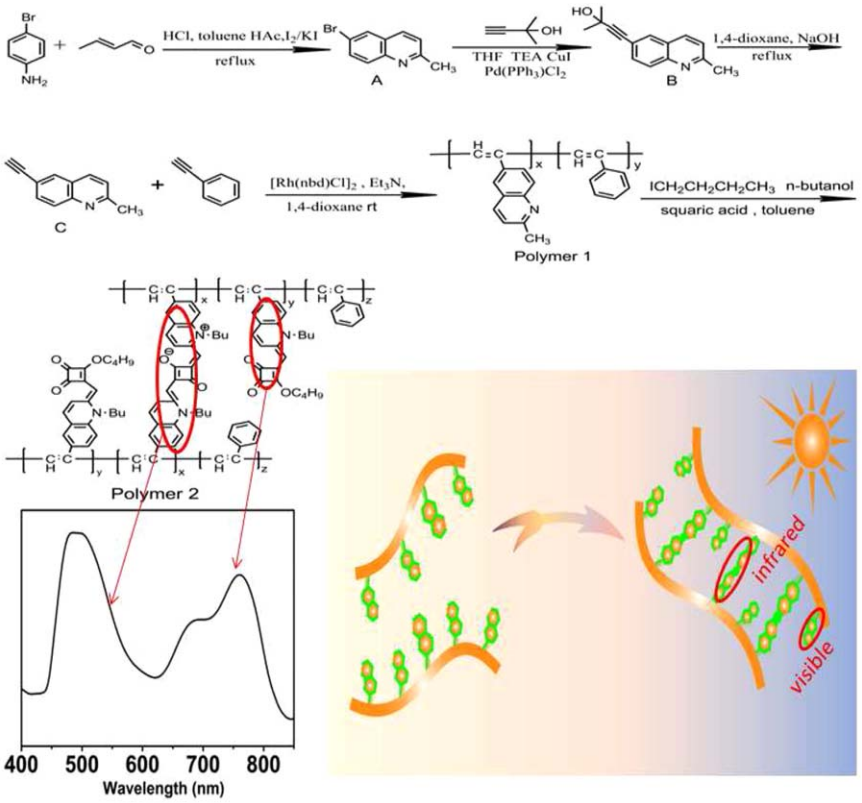

Figure 1. Schematic illustration of the synthesis and fabrication of the polyacetylene with broadband absorption. [Color figure can be viewed in the online issue, which is available at wileyonlinelibrary.com.]

molecular weight, but also effectively improves the solubility of the target polymer. The polymerization dynamics and formation mechanism of the broadband absorption properties were investigated by an online spectrum tracking method.

EXPERIMENTAL

Materials

Cuprous iodide, crotonaldehyde, iodine, 4-bromoaniline, potassium iodide, sodium hydroxide, sodium, anhydrous magnesium sulfate, 1,4-dioxane, triphenylphosphine dichloride palladium, toluene, glacial acetic acid, triethylamine, ether, hydrochloric acid, anhydrous ethanol, petroleum ether, ethyl acetate, tetrahydrofuran, methylene chloride, and 2-methylene-3-butylacetylene-2-alcohol were purchased from Shanghai Chemical Reagent Company, shanghai. Tetrahydrofuran, triethylamine, 1,4-dioxane, and crotonaldehyde were distilled prior to use.

Techniques

Fourier transform infrared (FTIR) spectra were recorded using a KBr disk on a Nicolet, Beijing NEXUS 8700 FTIR spectrometer. The ^{1}H-NMR spectra were collected on a Bruker, Switzerland DMX-400 spectrometer using chloroform-d ($CDCl_3$). The optical properties of the sample were measured by a Shimadzu, Germany UV-265 spectrometer with a 1-cm quartz cell. TGA (thermogravimetric analysis) was performed on a Perkin-Elmer, Shanghai TGA under an N_2 atmosphere at a heating rate of 10 °C min^{-1}. Elemental analyses were performed using a CHNOS Elemental Analyzer, Germany. The molecular weights of the polymers were estimated by gel permeation chromatography (GPC) with a Waters 510 high-performance liquid chromatography pump, a Rheodyne 7725i injector with a stand kit, a set of Styragel columns (HT3, HT4, and HT6; molecular weight range 102–107), a column temperature controller, a Waters 486 wavelength tunable ultraviolet-visible detector, a Waters 410 differential refractometer, and a system Dynamic Analysis Method (DMM)/scanner possessing an eight-channel scanner option. All of the polymer solutions were prepared in tetrahydrofuran (THF, ~2 mg mL^{-1}) and filtered through 0.45-μm poly(tetrafluoroethylene) syringe-type filters before injection into the GPC system. THF was used as the eluent as a flow was maintained at 30 °C, and the working wavelength of the UV detector was set at 254 nm. A set of monodisperse polystyrene standards was used for calibration.

Synthesis Procedures

Synthesis of 2-Methyl-6-Bromine-Quinoline (A). 4-Bromoaniline (6.136 g, 35.68 mmol), which was dissolved in H_2O (90 mL) and HCl (90 mL), was added to a 250-mL three-necked, round-bottom flask at 95 °C. After being dissolved, glacial acetic acid (2 mL) was added, and then crotonaldehyde (7.92 mL, 96.17 mmol) and toluene (24 mL) were added slowly and stirred for 8 h at 105 °C. The solution was stratified when the reaction was over. Finally, NaOH was added to the solution until the reaction system turned alkaline with pale yellow precipitates generated simultaneously. The solvent was distilled under reduced pressure, and the residue was purified by column

chromatography on silica gel (ethylacetate:petroleum ether = 1:6) to afford a brown solid in 80% yield.

FTIR (KBr) cm^{-1}: 3010 (C—H), 2950 (CH_3), 1370 (C—CH_3), 1600, 1500, 887 (quinoline C—C), 630 (C—Br).

^{1}H-NMR ($CDCl_3$): δ8.22 (1H, d, J = 8.4 Hz, 2-H), δ7.96 (1H, d, J = 3.4 Hz, 3-H), δ7.28 (1H, d, J = 8.6 Hz, 1-H), δ7.15 (1H, m, J = 3.5 Hz, 5-H), δ7.03 (1H, d, J = 8.4 Hz, 4-H), δ2.64 (3H, s, 7-H).

Elemental analysis ($C_{10}H_8NBr$): C, 54.48; H, 3.63; N, 6.33 (calculated: C, 54.08; H, 3.63; N, 6.3 for $C_{10}H_8NBr$).

Synthesis of 2-Methyl-6-(2-methyl-3-butyn-2-ol)-Quinoline (B). First, 2-methyl-6-bromine-quinoline (0.222 g, 1 mmol), alkynol (0.343 mL), tetrahydrofuran (10 mL) as solvent, triethylamine (5 mL) as acid agent, $PdCl_2(PPh_3)_2$ (0.0315g, 0.044 mmol), and CuI (0.0019 g, 0.01 mmol) as catalyst were added to a 100-mL three-necked, round-bottom flask under a nitrogen atmosphere, then heated to 70 °C for 40 h in a reflux condition, and a brown oily liquid was observed. The solution was cooled down to room temperature, methylene chloride and distilled water were added, and then the solution was filtered through a Buchner funnel. The solution was evaporated, and the product was purified by column chromatography with ethylacetate and petroleum ether (1:1) as eluting agent; a faint yellow crystal powder was obtained in 90.9% yield.

FTIR (KBr) cm^{-1}: 3200 (O—H), 3010 (C—H), 2950 (CH_3), 2250 (C≡C), 1370 (C—CH_3), 1600, 1500, 887 (quinoline), 1300 (C—OH).

^{1}H-NMR (DMSO): δ8.22 (1H, d, J = 8.4 Hz, 2-H), δ8.00 (1H, d, J = 1.4 Hz, 3-H), δ7.86 (1H, d, J = 8.6 Hz, 1-H), δ7.63 (1H, m, J = 3.4 Hz, 5-H), δ7.43 (1H, d, J = 8.4 Hz, 4-H), δ5.53 (1H, s, —OH), δ2.64 (3H, s, 7-H), δ1.50 (6H, s, —$(CH_3)_2$).

Elemental analysis: C, 79.23; H, 6.68; N, 6.05 (calculated: C, 79.96; H, 6.71; N, 5.58 for $C_{15}H_{15}NO$).

Synthesis of 6-Ethynyl-2-Methylquinoline (C). First, 2-Methyl-6-(2-methyl-3-butyn-2-ol)-quinoline (0.1126 g, 0.5 mmol), NaOH (0.2 g, 5 mmol), and 1,4-dioxane (20 mL) as solvent were added to a 100-mL three-necked, round-bottom flask, then heated to 80 °C for 8 h in a reflux condition. After the solution was cooled to room temperature, the solvent was distilled under reduced pressure to obtain a residue that was purified by column chromatography on a silica gel (ethylacetate:petroleum ether = 1:2) to afford a pale yellow solid in 85% yield.

FTIR (KBr) cm^{-1}: 3190 (C≡C—H, 2920 (CH_3), 2850 (C—H), 2100 (C≡C), 1370 (C—CH_3), 1600, 1490, 887 (quinoline C—C), 890, 840 (C—H).

^{1}H-NMR ($CDCl_3$): δ7.99 (1H, m, J = 8.4 Hz, 2-H), δ7.95 (1H, s, 3-H), δ7.73 (1H, m, J = 3.5 Hz, 1-H), δ7.31 (1H, d, J = 8.4 Hz, 5-H), δ7.20 (1H, s, 4-H), δ3.17 (1H, s, —C≡CH), δ2.75 (3H, s, 7-H).

Elemental analysis: C, 85.90; H, 5.41; N, 8.26 (calculated: C, 86.05; H, 5.43; N, 8.38 for $C_{12}H_9N$).

Synthesis of P 1. First, 6-ethynyl-2-methylquinoline (137 mg, 1 mmol), phenylacetylene (5.10 mg, 5 mmol), 1,4-dioxane (5.0 mL), $[Rh(nbd)Cl]_2$ (2.30 mg, 5.0×10^{-3} mmol) and Et_3N (1.01 mg, 5.0×10^{-2} mmol) dissolved in 1,4-dioxane (3.0 mL) were added in a 10-mL polymerization tube with side-arm Schlenk through vacuum nitrogen three times to keep an inert atmosphere and stirred for 5 h at room temperature. Then 1,4-dioxane (2.5 mL) containing a small amount of methanol solution was injected to terminate the reaction. The diluted solution was added to methanol (200 mL) to precipitate the product. Then the precipitate was collected and dissolved in a small amount of THF and added to methanol for purification. Such a dissolution–precipitation process was repeated until polymers free of unreacted monomers were obtained. Finally, the polymerization product was isolated and dried under vacuum at 40 °C to constant weight. In our study, it was found that the best solubility of the product is in a proper molar ratio of 1:5 for the 6-ethynyl-2-methylquinoline to phenylacetylene. The red-yellow powder product was obtained with a yield of 68%, which contains 18.2% 6-ethynyl-2-methylquinoline in the resultant copolyacetylene.

FTIR (KBr) cm^{-1}: 3022, 3053 (C=C—H), 1370 (C—CH_3), 1597, 1490, 888 (quinoline C—C), 890, 835 (C—H), 749, 698 (Ar—H).

^{1}H-NMR ($CDCl_3$): δ7.60–6.19 (quinoline —H, Ar—H); δ6.03–5.62 (C=C—H); 2.92–2.23 (—CH_3).

$$M_w = 1.68 \times 10^4, D = 2.09.$$

Synthesis of P 2. First, P 1 (861 mg, 1 mmol reactive groups), squaric acid (45.6 mg, 0.4 mmol), *n*-butanol (50 mL), iodobutane (0.55 g, 3 mmol), and toluene (7.5 mL) were added to a 100-mL three-necked, round-bottom flask in a reflux condition. The UV–visible absorption spectrum was used to track the reaction at different reaction times from 0 h to 40 h. The solution color gradually turned to red and finally become greenish. The solution was cooled down to room temperature, filtered, and then washed with deionized water to remove the squaric acid. Finally, a brown-red product was obtained.

FTIR (KBr) cm^{-1}: 3052 (=C—H), 1651 (C=C), 3022, 2957, 2926 (C—H), 1591, 1495, 885 (Ar), 1754 (C=O), 1321 (N—CH_2), 1164 (O—C—C).

^{1}H-NMR ($CDCl_3$): δ8.03–6.10 (Ar—H), δ5.80 (C=C—H), δ5.01 (C=CH—C), δ3.31 (N—CH_2—, C=CH—C), δ1.94 (—CH_2CH_2—), δ0.84 (—CH_3).

$$M_w = 3.92 \times 10^4, D = 1.89.$$

RESULTS AND DISCUSSION

In our work, it was found that the poly(6-ethynyl-2-methylquinoline) component is insoluble in some common solvents, such as THF and dioxane, which creates great difficulty for molecular structure characterization and also greatly limits their application research. In order to get the desired soluble polymer, we tried to copolymerize the 6-ethynyl-2-methylquinoline with phenylacetylene. Surprisingly, it was found that the trapezoidal squaraine polyacetylene is completely soluble when the feed ratio of 6-ethynyl-2-methyl-quinoline is less than or equal to 25 mol %. Thus, we first prepare poly[2-methyl-6-(5-phenyl-hexa-2,4-dien-3-yl)quinoline] using quinoline alkyne to phenyl

acetylene at molar feed ratio of 1:5. The chain structure ratio of the quinoline alkyne is at 18.2 mol % in the resultant poly(6-ethynyl-2-methylquinoline-*co*-phenyl-acetylene) with $M_w = 1.68 \times 10^4$ and $D = 2.09$. Thus, in the following work, the poly[2-methyl-6-(5-phenylhexa-2,4-dien-3-yl)quinoline] [abbreviated as poly(MAQ0.18-*co*-PA0.82) or P 1] was used as a raw polymer for the preparation of P 2 with near-infrared absorption.

In our previous work,[31] it is well known that semi-squaraine shows absorption in the visible region from about 400 nm to 600 nm, and squaraine displays absorption in the longer wavelengths from about 600 nm to 850 nm. In the synthesis of P 2, it is found that only semi-squaraine was yielded at the beginning. The squaraine significantly possesses an absorption peak when the reaction time was more than 10 h. The P 2 with suitable broadband absorption is shown at about 40 h. Simultaneously, the resulting P 2 is completely soluble in common solvents such as THF and DMSO. Thus, the structure characterization and optical measurement can be achieved by a general spectral technique. The molecular weight of P 2 was also evaluated by a gel permeation chromatography technique to be $M_w = 3.92 \times 10^4$ and $D = 1.89$, which is twice the average molecular weight of P 1. It can be predicted that the P 2 may possess a trapezoidal structure instead of a crosslinking network structure, which is further supported by the good solubility and the lower distribution of the molecular weight. Thus, we reach the conclusion that the resulting P 2 mainly exhibits a trapezoidal molecular structure.

Figure 2 shows the infrared spectra of 6-ethynyl-2-methylquinoline, P 1, and P 2. As can be seen in Figure 2, 6-ethynyl-2-methylquinoline clearly exhibits two characteristic absorptions at 3190 cm^{-1} and 2100 cm^{-1}, corresponding to the ≡C—H stretching vibration and —C≡C— absorption peaks, respectively.[32,33] However, these peaks disappear, and the new characteristic stretching vibration absorption bands at 3020 cm^{-1} and 3053 cm^{-1} belonging to =C—H appear in the FTIR spectrum of P 1. Peaks at 1600 cm^{-1}, 1490 cm^{-1}, and 1887 cm^{-1} for the —C=C— and —C—N— characteristic absorptions of quinoline and phenylacetylene are observed in P 1,[34] hinting that the quinoline acetylene has copolymerized with phenylacetylene. In the FTIR spectrum of P 2, the characteristic peaks at 1754 cm^{-1} and 1164 cm^{-1} corresponding to the C=O vibration peak in squaraine and the C—O—C vibration peak of semi-squaraine, respectively, have been observed, demonstrating that squaric acid reacted with the quinoline ring and that squaraine and semi-squaraine still exist in P 2. Generally speaking, the peaks at 3016 cm^{-1}, 2953 cm^{-1}, and 2872 cm^{-1} can be attributed to the C—H vibration peak in a flexible chain. In addition, the characteristic peaks located at 1616 cm^{-1}, 1581 cm^{-1}, and 1449 cm^{-1} could be indexed to the vibration absorption peak for the hydrogen skeleton of the benzene ring.

Figure 3 shows the ^{1}H-NMR spectra of 6-ethynyl-2-methylquinoline, P 1, and P 2 in chloroform-d. The single peak at 3.16 ppm corresponds to the alkyne proton in the 6-ethynyl-2-methylquinoline (C). Meanwhile, the signals at δ7.95 ppm, δ7.90 ppm, δ7.87 ppm, δ7.66 ppm, and δ7.24 ppm correspond to the protons of the quinoline ring in different positions, and the δ2.71 ppm absorption peak belongs to the three protons of

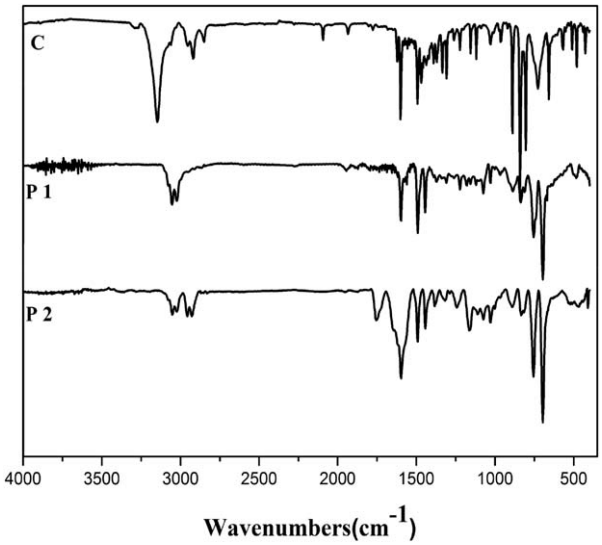

Figure 2. FTIR spectra of compounds 6-ethynyl-2-methylquinoline (C), P 1, and P 2.

the methyl group of 6-ethynyl-2-methylquinoline. It can be seen from the ^{1}H-NMR spectrum of P 1 that the characteristic absorption peak at 3.16 ppm corresponding to the alkyne proton disappears, and a new strong absorption peak at δ5.79 ppm belonging to the olefin proton absorption of the C=C band appears, demonstrating that C≡C has been changed into the configuration of C=C in the main chain. The proton absorption peaks corresponding to the quinoline ring at δ7.95 ppm, δ7.90 ppm, δ7.87 ppm, δ7.66 ppm, and δ7.24 ppm were significantly widened after forming the polymer compared to that of quinoline acetylene. The new peaks located at δ6.57 ppm and δ6.89 ppm correspond to the proton peaks of the quinoline ring and the benzene ring, respectively. The C—methyl proton peak in the quinoline ring at δ2.71 ppm becomes wide and shifts to δ2.64 ppm. The ratio of quinoline alkyne and phenylacetylene in the polymer structure can be evaluated to be 1:4.5

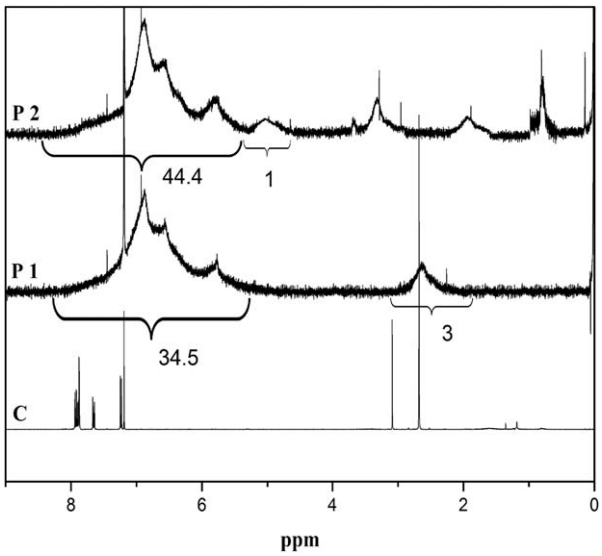

Figure 3. ^{1}H-NMR spectrum of compounds C, P 1, and P 2.

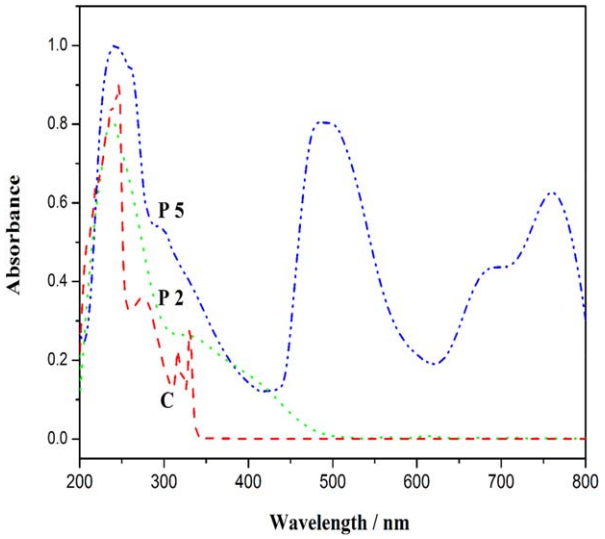

Figure 4. UV–vis absorption spectra of compounds C, P 1, and P 2. [Color figure can be viewed in the online issue, which is available at wileyonlinelibrary.com.]

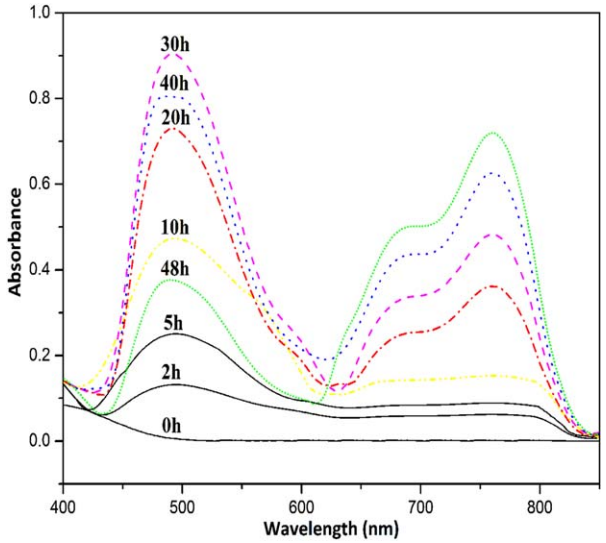

Figure 5. UV–vis absorption spectra obtained at various time intervals. [Color figure can be viewed in the online issue, which is available at wileyonlinelibrary.com.]

through the area integration of the proton peak in the resulting polymer (see Affix 1 in the Supporting Information), which has a 18.2% chain segment structure of quinoline alkyne, hinting that quinoline alkyne possesses better reaction activity than quinoline acetylene. It can be seen from the spectrum of P 2 that the *N*-methyl proton peak in the quinoline ring disappears, and a new peak at δ5.02 ppm corresponding to the bridge bond C═CH— proton peak in semi-squaraine and squaraine was exhibited in the ^{1}H-NMR spectrum of P 2. Simultaneously, the proton absorption peaks at δ3.32 ppm, δ1.95 ppm, and δ0.81 ppm belonging to the α-methene, β,γ-methene, and end methyl proton peaks for the N^{+}—Bu and —O—Bu groups in semi-squaraine and squaraine, and the α-methene, β,γ-methene, and end methyl proton peaks of N^{+}—Bu in squaraine were obviously observed in the ^{1}H-NMR spectrum of P 2, respectively. The —OCH_2— unit resonance peak is located at δ3.5 ppm. The ratio of semi-squaraine to squaraine in P 2 can be evaluated to be 1:0.14 based on the calculation of the proton peak area integration (see Affix 2 in the Supporting Information).

Figure 4 shows the typical UV–vis absorption spectra of 6-ethynyl-2-methylquinoline, P 1, and P 2 in THF. First, the standard solution concentration of 6-ethynyl-2-methylquinoline, P 1, and P 2 in THF is 1×10^{-3} mol/L. However, they were diluted to 2×10^{-5} mol/L when they were characterized in UV–vis absorption. It can be seen from Figure 4 that the 6-ethynyl-2-methylquinoline displays a strong absorption peak at 247 nm, which is assigned to the quinoline ring. Additionally, the weaker absorption peak at 270 nm belongs to the n→π* transition. The absorption peaks located at 316 nm and 332 nm in 6-ethynyl-2-methylquinoline originate from the conjugation effect of the quinoline ring and the alkynyl group. The two absorption peaks of 6-ethynyl-2-methylquinoline located at 316 nm and 332 nm disappeared after being polymerized into P 1, and a new shoulder peak at about 400 nm belonging to the conjugated main chain of polyacetylene was exhibited in the UV–vis absorption spectrum for P 1. Interestingly, in the absorption spectrum of P 2, it is surprisingly found that a strong broadband absorption from 440 to 900 nm with maximum absorption peaks at 495 nm, 680 nm, and 750 nm was observed.[35] It is well known from our previous work that the maximum absorption peak at 495 nm is attributed to the cshar-acteristic absorption of semi-squaraine itself, and the maximum absorption peaks at 680 nm and 750 nm belong to the characteristic absorption of squaraine itself. The results further support that the P 2 was yielded with broadband absorption, which is consistent with the results from the FTIR and ^{1}H-NMR spectra.

To investigate the formation mechanism of P 2, an online tracking technique was carried out. Figure 5 presents the dynamic UV–vis spectra of the reaction system at different times. As can be seen from Figure 4 for P 1 and Figure 5 (curve at 0 h), the raw material has almost no absorption at more than 500 nm. After a reaction time of 2 h, a small absorption peak at 495 nm and a very weak and broad absorption ranging from 635 to

Table I. Concentrations of Semi-squaraine and Squaraine at Different Reaction Times

Reaction time (h)	0	2	5	10	20	30	40	48
Concentration of semi-squaraine ($\times 10^{-5}$ mol L^{-1})	0	0.45	0.86	1.62	2.47	3.06	1.25	1.07
Concentration of squaraine ($\times 10^{-5}$ mol L^{-1})	0	0	0.02	0.03	0.08	0.11	0.14	0.16
Total concentration of semi-squaraine ($\times 10^{-5}$ mol L^{-1})	0	0.45	0.88	1.65	2.55	3.17	1.39	1.23

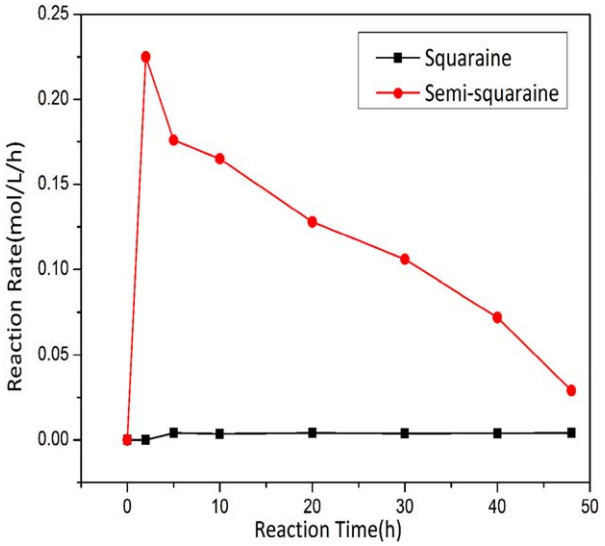

Figure 6. Reaction rates at various time intervals. [Color figure can be viewed in the online issue, which is available at wileyonlinelibrary.com.]

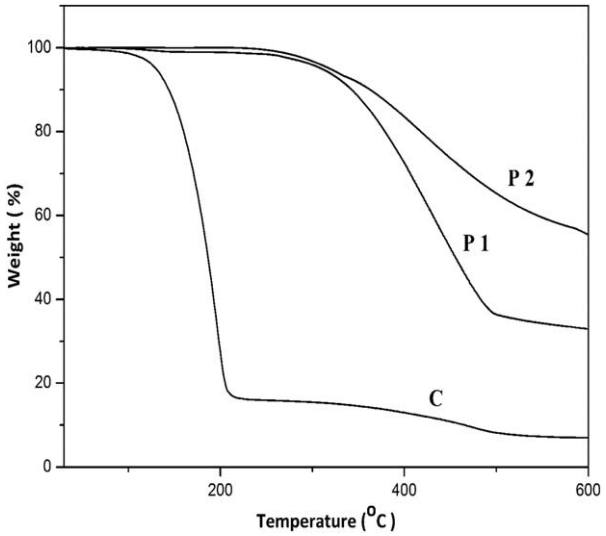

Figure 7. TGA curves of compounds C, P 1, and P 2.

850 nm were observed, which belong to the characteristic peaks of the semi-squaraine and squaraine groups themselves, respectively.[33] The absorption peak at 495 nm assigned to semi-squaraine gradually increased as the reaction progressed and reached a maximum value at a reaction time of about 30 h; no absorption peak at 680 nm or 750 nm was found when the reaction time was less than 10 h. The strong absorption peaks at 680 nm and 750 nm, which belong to squaraine, was observed at a reaction time of about 20 h. This demonstrates that semi-squaraine was formed first and squaraine was quickly generated after reaching a certain concentration of semi-squaraine. That is, a dynamic equilibrium was shown in the formation process of P 2. Simultaneously, it was also found that a suitable broadband absorption for P 2 was obtained at about 40 h. Based on the Beer–Lambert law and the molar absorption coefficients of semi-squaraine and squaraine from the relevant monomers, the critical concentration of squaraine generated is about $1.65 \times 10^{-}+$ mol L^{-1} (the molar absorption coefficients of the relevant monomer semi-squaraine and squaraine are 2.91×10^4 L mol^{-1} cm^{-1} and 4.42×10^5 L mol^{-1} cm^{-1}; see Affix 3 in the Supporting Information). The concentrations of semi-squaraine and squaraine in the reaction system at different times were also calculated as the reaction progressed based on the absorption spectra. The results are shown in Table I.

Table I shows the dynamical concentrations of semi-squaraine and squaraine at various times. It can be seen from Table I that the concentration of semi-squaraine was first increased with time and decreased after reaching a maximum concentration significantly. At the same time, the concentration of squaraine was increased in a step-by-step manner (Figure 1).

Thus, the reaction activation energy can be represented to be the difficulty level for the reactive molecule to change into an activated molecule based on the Arrhenius equation: $k = Ae^{-Ea/RT}$), where k is the constant of reaction rate, A is a frequency factor, Ea is the activation energy of the reaction system, and $R = 8.314$ J mol^{-1} K^{-1}. Then, based on Figure 6 and Table I, we can infer that the reaction rate constant of semi-squaraine is larger than that of squaraine. According to the Arrhenius equation, we may safely draw the conclusion that the activation energy of squaraine is greater than that of semi-squaraine. So, in the reaction system, semi-squaraine was generated first. This is consistent with the result from the reaction process.

The thermal stability of optical materials is one of the most important factors in improving device lifetime and reliability. The thermal stability of the polymers was evaluated by TGA, and Figure 7 depicts the TGA curves of 6-ethynyl-2-methylquinoline, P 1, and P 2 under nitrogen at a heating rate of 10 °C min^{-1}. The thermal decomposition temperatures (T_d, 5 wt % loss) of 6-ethynyl-2-methylquinoline, P 1, and P 2 are 129 °C, 310 °C, and 319 °C, respectively. Simultaneously, the residue of P 2 was increased by nearly 20% over that of P 1 when the temperature was increased to 600 °C. P 2 shows better thermal stability than P 1, which may be attributed to the trapezoidal structure of the resulting P 2 and a strong dipolar interaction between the squaraine groups.

CONCLUSIONS

A soluble trapezoidal polyacetylene with broadband absorption was successfully fabricated via simply controlling the reaction time in a one-step strategy. The results indicate that the functional trapezoidal polyacetylene has a better solubility due to the copolymerization with phenylacetylene, and the enhancement of thermal stability may originate from the trapezoidal structure.

ACKNOWLEDGMENTS

This research was financially supported by the National Natural Science Fund of China (Grant Nos. 21471030, 21271040, and 21171034), the Shanghai Municipal Natural Science Foundation for Youths (No. 12ZR144100), and the "Chen Guang" project

(No. 12CG37), supported by the Shanghai Municipal Education Commission and the Shanghai Education Development Foundation.

REFERENCES

1. Ji, Y.; Feng, X.; Xiao, C. C.; Dong, Y. F.; Wang, Q. Z.; Wang, M.; Zhao, Y. Y. *Chin. Chem. Lett.* **2010**, *21*, 850.
2. Lu, W.; Zheng, G. R.; Shen, J. S.; Cai, J. C. *Chin. Chem. Lett.* **1999**, *10*, 201.
3. Kajzar, F.; Etemad, S.; Baker, G. L.; Messier, J. *Solid State Commun.* **1987**, *63*, 1113.
4. Fann, W. S.; Benson, S.; Madey, J. M. J.; Etemad, S.; Baker, G. L.; Kajzar, F. *Phys. Rev. Lett.* **1989**, *62*, 1492.
5. Takahashi, A. *Synth. Met.* **1997**, *85*, 1087.
6. Lam Jacky, W. Y.; Qin, A. J.; Dong, Y. Q.; Hong, Y. N.; Jim Cathy, K. W.; Liu, J. Z.; Dong, Y. P.; Kwok, H. S.; Tang, B. Z. *J. Phys. Chem.* **2008**, *112*, 11227.
7. Vicente, J.; Gil-Rubio, J.; Zhou, G. J.; Bolink, H. J. *J. Polym. Sci., Part A: Polym. Chem.* **2010**, *48*, 3744.
8. Robinson, S. G.; Johnston, D. H.; Weber, C. D.; Lonergan, M. C. *Chem. Mater.* **2010**, *22*, 241.
9. Metzger, B. T.; Barnes, D. M. *J. Agric. Food Chem.* **2009**, *57*, 11134.
10. Cheuk, K. K. L.; Li, B. S.; Lam Jacky, W. Y.; Xie, Y.; Tang, B. Z. *Macromolecules* **2008**, *41*, 5997.
11. Yin, S. C.; Xu, H. Y.; Li, G.; Su, X. Y. *J. Polym. Sci.* **2006**, *24*, 221.
12. Yu, Z. Q.; Lam Jacky, W. Y.; Zhao, K. Q.; Zhu, C. Z.; Yang, S.; Lin, J. S.; Li, B. S.; Liu, J. H.; Tang, B. Z. *Polym. Chem.* **2013**, *4*, 996.
13. Daniel, G. *Bonding* **1999**, *95*, 41.
14. Chandrasekhar, S.; Ranganath, G. S. *Rep. Prog. Phys.* **1990**, *53*, 57.
15. Kim, H. S.; Lee, J. H.; Kim, T. H.; Okabe, S.; Shibayama, M.; Choi, S. M. *J. Phys. Chem. B* **2011**, *115*, 7314.
16. Ariza-Carmona, L.; Martin-Romero, M. T. *J. Phys. Chem. C* **2013**, *117*, 21838.
17. Su, X. Y.; Xu, H. Y.; Yang, J. Y.; Lin, N. B.; Song, Y. L. *Polymer* **2008**, *49*, 3722.
18. Wang, X.; Wu, J. C.; Xu, H. Y.; Wang, P.; Tang, B. Z. *J. Polym. Sci. Polym. Chem.* **2008**, *46*, 2072.
19. Wang, X.; Yan, Y. X.; Liu, T. B.; Su, X. Y.; Qian, Y. L.; Xu, H. Y. *J. Polym. Sci. Polym. Chem.* **2010**, *48*, 5498.
20. San Jose, B. A.; Matsushita, S.; Akagi, K. *J. Am. Chem. Soc.* **2012**, *134*, 19795.
21. San Jose, B. A.; Matsushita, S.; Moroishi, Y.; Akagi, K. *Macromolecules* **2011**, *44*, 6288.
22. Ding, L.; Huang, Y. Y.; Zhang, Y. Y.; Deng, J. P. *Macromolecules* **2011**, *44*, 736.
23. Maeda, K.; Wakasone, S.; Shimomura, K.; Ikai, T.; Kanoh, S. *Macromolecules* **2014**, *47*, 6540.
24. Li, W. F.; Wang, B.; Yang, W. T.; Deng, J. P. *Rapid Communications* **2015**, *36*, 319.
25. Lin, N. B.; Feng, Y.; Guang, S. Y.; Xu, H. Y. *Chin. Chem. Lett.* **2011**, *22*, 1257.
26. Zhang, H. Y.; Qian, Q. G.; Song, J. X.; Deng, J. P. *Ind. Eng. Chem. Res.* **2014**, *53*, 17394.
27. Ajayaghosh, A.; Arunkumar, E. *Org. Lett.* **2005**, *7*, 3135.
28. Wallace, K. J.; Gray, M.; Zhong, Z. L.; Lynch, V. M. *Dalton. Trans.* **2005**, *14*, 2436.
29. Ajayaghosh, A.; Chithra, P.; Varghese, R.; Divya, K. P. *Chem. Commun.* **2008**, *8*, 969.
30. Chung, S. J.; Zheng, S. J.; Odani, T.; Beverina, L.; Fu, J.; Padilha, L. A.; Biesso, A.; Hales, J. M.; Zhan, X. W. *J. Am. Chem. Soc.* **2006**, *128*, 14444.
31. Lee, W.; Min, S. K.; Cai, G.; Mane, R. S.; Ganesh, T.; Koo, G. *Electrochim. Acta* **2008**, *54*, 714.
32. Yan, Z. Q.; Guang, S. Y.; Su, X. Y.; Xu, H. Y. *J. Phys. Chem. C* **2012**, *116*, 8894.
33. Maeda, T.; Nitta, S.; Nakao, N.; Yagi, S.; Nakazumi, H. *J. Phys. Chem. C* **2014**, *118*, 16618.
34. Yan, Z. Q.; Xu, H. Y.; Guang, S. Y.; Zhao, X.; Fan, W. L.; Liu, X. Y. *Adv. Funct. Mater.* **2012**, *22*, 345.
35. Wang, X.; Yan, Y. X.; Liu, T. B.; Su, X. Y.; Qian, L. W.; Song, Y. L.; Xu, H. Y.; *J. Polym. Sci., Part A: Polym. Chem.* **2010**, *48*, 5498.